REPORT 303

ADVISORY GROUP FOR AERONAUTICAL RESEARCH AND DEVELOPMENT

64 RUE DE VARENNE, PARIS VII

REPORT 303

TUNNEL-WALL EFFECTS ASSOCIATED WITH VTOL-STOL MODEL TESTING

by

R. E. KUHN and R. L. NAESETH

MARCH 1959

NORTH ATLANTIC TREATY ORGANISATION

REPORT 303

NORTH ATLANTIC TREATY ORGANIZATION

ADVISORY GROUP FOR AERONAUTICAL RESEARCH AND DEVELOPMENT

TUNNEL-WALL EFFECTS ASSOCIATED WITH VTOL-STOL MODEL TESTING

by

Richard E. Kuhn and Rodger L. Naeseth

This Report is one in the Series 292-305, inclusive, of papers presented at the Interference Effects Meeting of the AGARD Fluid Dynamics Panel (formerly Wind Tunnel and Model Testing Panel) held 2-5th March 1959, at the Training Center for Experimental Aerodynamics, Rhode St. Genèse, Belgium

SUMMARY

Wind-tunnel investigations of VTOL (vertical take-off and landing) and STOL (short take-off and landing) airplane models involve configurations in which a large amount of power is being used to generate part of the lift through the medium of propeller slipstreams or jet exhausts directed downward at large angles to the free-stream direction. For many configurations the propellers or jet exhausts are arranged, for example, as in the jet flap, to cover the entire span of the wing and thus to assist the wind in its natural process of producing so-called 'circulation' lift. This arrangement results in the streamlines in the vicinity of the wing also being turned through large angles to the free-stream direction of flow. The presence of the tunnel walls, however, imposes the conditions that the streamlines at the tunnel walls must be parallel to the free stream. Thus, the problem of tunnel-wall effects in VTOL-STOL model testing is similar to that associated with conventional model testing but differs greatly in degree. Experience has shown that, in addition to these usual tunnel-wall effects, flow separation on the model can also be induced by the tunnel walls. The experiences of the Langley Research Center of N.A.S.A. related to these problems in closed-throat wind tunnels are reviewed in this paper.

533.6.071.4:533.652.6.

3b8c7a:3b3k

SOMMAIRE

Des mesures effectuées en soufflerie sur des maquettes VTOL et STOL (à décollage et à atterrisage verticaux et courts) mettent en jeu des configuratious dans lesquelles une quantité importante de puissance s'emploie pour produire une partie de la sustentation nécessaire à l'aide de sillages d'hélice ou de tuyères d'échappement dirigés vers le bas à de grands angles à la direction de la veine libre. Pour beaucoup de configurations les hélices un les tuyères d'échappement sont disposés, par exemple, comme dans le cas des volets soufflés de facon à s'étendre sur toute l'envergure de l'aile, contribuant ainsi à aider l'aile dans son processus naturel de réaliser de la sustentation dite 'de circulation'. Cette disposition permet aux lignes de courant au voisinage de l'aile de se tourner également par de grands angles à la direction d'écoulement de la viene libre. Toutefois, la présence des parois de la soufflerie impose la condition qui exige que les lignes de courant aux parois de la soufflerie soient parallèles au courant libre. Ainsi, la problème des effets de paroi dans les essais effectués sur des maquettes VTOL/STOL est analogue à celui auquel se heurte l'essai de maquettes de type classique, sauf qu'il y a une différence de degré. L'expérience a montré que, en plus de ces efets de paroi de soufflerie, la séparation de l'écoulement peut être induite par les parois de la soufflerie. La rapport passe en revue les expériences du Langley Research Center de la NASA en ce qui concerne ces problèmes dans des souffleries à gorge fermée.

533.6.071.4:533.652.6

3b8c7a:3b3k

CONTENTS

LIST OF FIGURES

NOTATION

C_L	lift coefficient (Lift/qS)
C'_L	lift coefficient of ducted-fan model (Lift/¼πqd²)
C_D	drag coefficient (Drag/qS)
C'_D	drag coefficient of ducted-fan model (Drag/¼πqd²)
C_T	thrust coefficient (T/qS)
C'_T	thrust coefficient of ducted-fan model (T/¼πqd²)
C_μ	jet momentum coefficient (wV_j/qS)
h	height above ground plane (ft)
D	propeller diameter (ft)
d	exit diameter of ducted fan (ft)
T	thrust (lb)
w	mass flow of jet (lb sec/ft)
$\bar{c}$	wing mean geometric chord (ft)
V_j	jet velocity (ft/sec)
S	wind area (ft²)
C	cross-sectional area of test section (ft²)
q	free-stream dynamic pressure ($\frac{1}{2}\rho V_0^2$ lb/ft²)
V_o	free-stream velocity (ft/sec)
ρ	density of air in free stream (slugs/ft³)
F	resultant force (lb)
θ	turning angle (deg)
ϕ	attitude with respect to tunnel center line (deg)
α	angle of attack (deg)
$\Delta\alpha$	increment of angle of attack calculated by conventional correction procedures (deg)
δ	test-section-boundary correction factor

TUNNEL-WALL EFFECTS ASSOCIATED WITH VTOL-STOL MODEL TESTING

Richard E. Kuhn* and Rodger L. Naeseth*

1. PROPELLER-POWERED CONFIGURATIONS

1.1 Static Investigations

The first experimental evidence encountered at the Langley Research Center of the seriousness of the tunnel-wall effects problem was obtained with a deflected-slipstream configuration in the Langley 300 mph 7 x 10 ft tunnel[1]. These tests attempted to measure the slipstream-deflection characteristics of a wing-flap configuration at zero forward speed in the test section of the tunnel. The model size would have been considered conventional for normal power-off testing. The semispan wing (Fig.1) was mounted from the tunnel ceiling and had a semispan area of 5.50 square feet, a semispan of 3.7 feet, and used two overlapping 2 ft diameter propellers. A curtain was installed in the diffuser behind the test section to prevent the development of an airflow around the circuit of the tunnel.

The results shown in Figure 2 indicate that the turning angle measured in the tunnel was as much as 10° less than that measured in a large (18.5 ft x 42.5 ft x 10 ft) room. Also, the losses in the turning process were increased by 10 to 15%. These losses are attributed directly to flow separation on the upper surface of the wing caused by the effects of the walls, notably the wall on which the slipstream impinges, in altering the direction of flow of the slipstream.

This effect is very similar to the ground effects on deflected slipstream configurations as indicated in Reference 2 and as shown schematically in Figure 3. When the slipstream leaving the model trailing edge strikes the ground or tunnel wall at an angle somewhat less than the vertical, as depicted in Figure 3 (which is usually the case for all except perhaps the highest flap deflections), most of it is deflected rearward, thereby making it harder to maintain the Kutta condition and increasing the likelihood of separation. The large decreases in turning angle in the negative attitude range of Figure 2 illustrate these effects. Also, when the slipstream strikes the ground or tunnel wall at or near the vertical the pressure-field set up causes the slipstream to spread with attendant deviations in flow direction and an increase in the adverse pressure gradient against which the slipstream must flow. These factors add to the others already present that tend to cause flow separation. Reference 2 indicates that these effects can be important at considerable distance from the ground or tunnel wall. In the tests shown in Figure 2 the distance from the trailing edge to the tunnel wall was only about 2 propeller diameters. Reference 2 indicates that a distance of 4 or 5 diameters is needed to be out of the region of ground effect for the hovering condition.

Of course, in the tunnel the other walls probably also contribute to the losses in that they restrict the space available for the slipstreams to recirculate. High-velocity flows along the tunnel walls are present and set up secondary flows that greatly influence the character of the results.

---

*National Aeronautics and Space Administration, Langley Research Center, Langley Field, Va., U.S.A.

Although no data were available for comparison at forward speeds, it was fairly obvious that these effects would also influence the data obtained at forward speeds. Inasmuch as flow separation was involved, it seemed improbable that reliable procedures for correcting the data could be devised, and it was decided instead that a test facility designed to avoid these problems would be needed. The facility developed is shown in Figure 4 and consisted of installing a special 17 ft test section in the entrance cone of the tunnel. Detailed discussion of this development and possible alternative schemes are presented in a subsequent section of this paper.

The work reported in Reference 2 had indicated that a test section of this size would be adequate for semispan models with semispans of 3 to 4 feet using propellers 2 feet in diameter or less. The data of Figure 5 were obtained in the 17 ft test section with the same model that was used in the 7 x 10 ft test section and verify that the 17 ft test section is adequate for models of this size.

Another problem of obtaining static data in a wind tunnel is also illustrated in Figure 5 by the comparison of the curves with the curtain in and with the curtain out. The curtain referred to here was installed across the 7 x 10 ft test section so as to eliminate the possibility of the model effectively 'powering' the tunnel and setting up an air flow around the circuit of the tunnel. With the curtain out, an air flow was set up; that is, a very slow forward-speed condition was simulated corresponding to a thrust coefficient of the order of $C_T \approx 200$. In order to obtain true static conditions in a wind tunnel, it is necessary to install a curtain or other blockage in the tunnel circuit to avoid this condition.

1.2 Transition-Speed-Range Investigations

A comparison of the data obtained at forward speeds in the 7 ft x 10 ft test section with that obtained in the 17 ft test section is presented in Figure 6. The tunnel-wall effects show up at the highest thrust coefficients and cause premature stalling of the models when tested in the 7 ft x 10 ft test section.

The conventional corrections for wall-induced upwash have been applied to the angle-of-attack and drag data of Figure 6 and also to the jet-flap data that are to be discussed subsequently. These corrections are proportional only to the circulation part of the lift and the direct-thrust contribution to the lift must be subtracted before these corrections are applied. The corrections take the familiar form

$$\alpha = \alpha_{measured} + \Delta\alpha$$

where

$$\Delta\alpha = 57.3\delta \frac{S}{C} C_{L,\Gamma}$$

and

$$C_D = C_{D_{measured}} + \delta \frac{S}{C} C_{L,\Gamma^2}$$

where the lift proportional to circulation is assumed to be given with reasonable accuracy, for the propeller-driven models, by

$$C_{L,\Gamma} = C_L - C_T \frac{F}{T} \sin(\theta + \alpha)$$

and, for the jet-flap models, by

$$C_{L,\Gamma} = C_L - C_\mu \frac{F}{w V_j} \sin(\theta + \alpha)$$

In these expressions F/T is the ratio of resultant force to propeller thrust under static conditions, F/wV_j is the ratio of resultant force to momentum thrust of the jet sheet under static conditions, and θ is the angle through which the slipstream or jet sheet is turned under static conditions.

The data for the deflected-slipstream configuration are presented with and without these corrections applied in Figure 6(c) and show that the errors in the data due to the classical induced upwash corrections are small compared with the effects of wall-induced separation.

The effects of wall-induced separation are similar to the ground effects experienced on other deflected-slipstream models. These ground effects appear as a premature stall and a decrease in maximum lift. Serious ground effects, however, do not appear until the model is closer to the ground ($h/D < 2.9$, Fig.7) than the corresponding wall of the tunnel ($h/D = 2.5$). The data of Figure 7 were obtained from the present model in the 17 ft test section with a ground board installed at various distances below the model. With the ground board installed at the same distance from the model as the corresponding wall of the 7 ft x 10 ft test section ($h/D = 2.5$), the data were only slightly affected. In fact, in the negative angle-of-attack range there appears to be a slight favorable ground effect of the type associated with the trailing vortex system. Clearly then, the tunnel wall 'below' the model is not the sole cause of the losses experienced.

The other tunnel walls, particularly the wall 'above' the model, alter the curvature of the streamlines around the model as shown schematically in Figure 8. If the tunnel walls were not present, the stream-lines would be approximately as shown by the dashed lines; however, the presence of the walls forces the streamlines at the walls to be straight, with the result that the entire field is altered somewhat as shown by the solid lines. This is, of course, the streamline-curvature effect treated in papers on conventional tunnel-wall effects; however, with high lift coefficients encountered on VTOL-STOL configurations this alteration of the streamlines apparently results in an increase in the adverse pressure gradient over the rear portion of the model sufficient to cause premature stall. The obvious ways to avoid these effects would be to move the walls out to a streamline that is almost straight, or to decrease the model size so that the streamline curvature that would normally be present at the position corresponding to the walls is no greater than exists under conventional conditions. The curvature of the streamlines is proportional to the circulation lift. Also, the incremental angle of attack ($\Delta\alpha$) calculated by conventional tunnel-wall correction procedures is proportional to the circulation. Thus, this calculated $\Delta\alpha$ can be used as an indirect indication of the extent of streamline curvature.

Anscombe and Williams[3] have suggested that the model size be chosen such that at the highest lift expected the calculated increment in angle of attack $\Delta\alpha$ due to wall-induced upwash should not exceed 2.0^{o}. The values of $\Delta\alpha$ reached at several points are indicated in Figure 6. While it would not be expected that a precise numerical value could be recommended, it appears that the suggested value of 2.0 is a reasonable guide with possibly slightly higher values permissible for tilt-wing configurations and slightly lower values desirable for highly flapped configurations.

2. JET-FLAP CONFIGURATIONS

A comparison of the data obtained with two jet-flap models tested in each test section is presented in Figure 9. The swept-wing model (Fig. 9a) was the larger of the two, and had a semispan area of 3.2 square feet and a semispan of 3.36 feet. Because of limitations of the air supply available, the maximum momentum coefficient that could be reached was 6.2. It was only at about this level of momentum coefficient that noticeable tunnel-wall effects appeared (Fig. 9a). Again, as with the propeller-driven models, the data obtained in the 7 ft × 10 ft test section indicate a premature break in the lift curve. This model was also tested in the 17 ft test section with a ground board installed at various distances below the model (Fig. 10). With the ground board installed at the same distance from the model as the corresponding wall of the 7 ft × 10 ft test section a slight favorable ground effect appears in the low and negative angle-of-attack range. However, at the lift break the data are very similar to those obtained in the 7 ft × 10 ft test section. Thus, it appears that, with jet-flap models, the wall 'below' the model is the primary contributor to the tunnel-wall effects. These effects appear to be due to the development of a forward flow along the tunnel wall that was observed at high angles of attack. The flow probably indicates the beginnings of a vortex flow under the wing of the type discussed in connection with jet-flap ground effects in Reference 4 and illustrated herein in Figure 11 (which was taken from Ref. 4).

Some indications of this type of vortex flow have also been observed with propeller-driven models in the region of ground effect. It is not possible, however, to determine how much of the lift losses is due to the observed flow separation from the flaps and wing upper surface and how much is due to this vortex flow under the wing. With the jet-flap models, however, the high-energy jet sheet flowing on the flap at least prevents separation from the flap.

In this connection, a practice that has frequently been used at the Langley Research Center as a guide to determining when wall effects might be becoming important has been to place yarn tufts on the wall of the tunnel 'below' the model in order to determine when the jet sheet actually impinges on this wall. Any indication from the tufts that an upstream flow is developing along the wall is usually viewed as an indication of trouble. In the case of the present swept-wing model at a C_{μ} of 6.2 (Fig. 9a), the tufts below the model generally indicated a strong spanwise outflow along the wall, below and behind the model, which was undoubtedly due in large measure to the trailing vortex system. The first indication of the development of an upstream component of flow along the wall developed at an angle of attack slightly below 20^{o}.

Data to higher momentum coefficients have been obtained by using a much smaller unswept-wing model. The model[5] had a semispan area of 1.5 square feet and a span of

2.5 feet. In general, these data (Fig. 9b) show slightly higher lifts and lower drags in the 7 ft × 10 ft test section at the higher momentum coefficients. This result may indicate a slight favorable ground effect such as that shown at low and negative angles of attack in Figure 10, or it may simply be a result of experimental inaccuracies. In any event these differences are small and would probably be considered to be of little consequence in most practical applications. Unfortunately, the tests at the higher momentum coefficients were terminated before the stall was reached so that it is not possible to determine the full extent of the wall effects at these high momentum coefficients.

The calculated angle-of-attack correction $\Delta\alpha$ due to induced upwash as computed by conventional procedures has been spotted on the jet-flap data of Figure 9 as was done with the propeller-powered models previously discussed. Also, as with the propeller-powered models, it appears that the suggested limiting value of 2.0 is a good guide.

3. DUCTED-FAN CONFIGURATION

The results of tests of a ducted fan in the two test sections are compared in Figure 12. The coefficients presented are based on the exit area of the fan, and the tests were run at constant fan rotational speed through the angle-of-attack range. Differences in the data are noted only at extremely high thrust coefficients. Because of the small size of the model (exit diameter of 15 inches, duct length of 13 inches) serious wall effects had not been expected. Note that at the highest thrust coefficient the calculated increment in angle of attack from conventional correction calculations is only 0.8°. The reasons for the small differences shown are not fully known; however, some observations concerning the results may be of value in assessing this comparison in the light of similar or perhaps future work. The model used was constructed so that the division of thrust between the fan and the shroud could be measured. These results indicate that the loss in lift shown in Figure 12 was due to changes in forces on the duct. The fan thrust did not change appreciably between the two test sections. This result probably indicates an increase in the extent of flow separation on the upper (or rearward, at $\alpha = 90^{\circ}$) lip of the duct when installed in the 7 ft × 10 ft test section.

4. DEVELOPMENT OF THE 17 FT TEST SECTION

In order to avoid the previously discussed tunnel-wall effects in tests of VTOL-STOL configurations it is necessary to use either a larger test section or smaller models. The decision at the NASA Langley Research Center to build a larger test section rather than smaller models was based on a number of considerations. First of all, smaller models would have resulted in very low Reynolds numbers. Also the problems of building powered models in very small sizes can be serious. Of equal or greater importance, however, was the need for very low and accurately controlled tunnel airspeeds to simulate the low-speed end of the transition speed range. Very low speeds are difficult to maintain in most tunnels. By installing a new large test section in the circuit of the Langley 300 mph 7 ft × 10 ft tunnel, it has been found possible to run tests at speeds as low as 10 ft/sec with reasonable accuracy by calibrating the flow in the large test section against the velocities measured in the 7 ft × 10 ft test section.

The Langley 300 mph tunnel fortunately had a relatively long settling chamber upstream of the entrance to the 7 ft × 10 ft tunnel test section. This made it possible to install the new larger test section just upstream of the original test section as shown in Figure 4. A photograph of the installation is shown in Figure 13. This view of the 17 ft test section is taken looking down stream and shows the original 7 ft × 10 ft tunnel test section in the background. A semispan model is shown with the ground board installed for ground effect tests. Also the freely floating vanes used to measure the average downwash in the region of the horizontal tail can be seen just behind the model. Installation of the 17 ft test section did not impair the usefulness of the 7 ft × 10 ft test section.

The lines of the 17 ft test section were developed from tests in a 1/8-scale model tunnel. Initial tests indicated a very pronounced velocity gradient (velocities increasing with distance downstream) at the center line with all walls parallel to the center line. This gradient made it necessary to increase the divergence on the side walls (floor and ceiling were kept level for convenience) much beyond the divergence that would be required to compensate for boundary-layer growth. A wall-divergence angle of 2.5° to the tunnel center line was found satisfactory. The designation '17 ft' for the test section is an arbitrary designation used for convenience. The actual height is 15.75 ft and the width at the model location is 17.2 ft.

The test section was installed with the lines indicated by the model tunnel tests and subsequent calibration indicated excellent agreement with the model tunnel predictions. The dynamic-pressure distributions in the vertical plane through the tunnel center line are shown in Figure 14. The reductions in dynamic pressure near the floor at downstream locations is a direct result of large divergence required to obtain the flat center-line distribution shown.

Surveys of the flow in vertical planes 4 feet on either side of the center line indicate dynamic-pressure contours almost identical to that shown in Figure 14. The available test region is therefore at least 8 feet wide and about 12 feet long on the tunnel center line. It is somewhat shorter for floor-mounted semispan models, because of the reduced dynamic pressures in the downstream regions.

Two types of model supports are provided, both using strain-gage balance installations. A strut support system is available for complete models. The strut length can be changed to allow testing at a low position near the tunnel floor for ground effect investigations. Semispan models are mounted on a turntable in the tunnel floor which also serves to yaw the strut support system for lateral directional tests of complete models.

Most low-speed wind tunnels, unfortunately, do not have a long settling chamber ahead of the entrance cone. In these tunnels another location at some point in the return passages of the tunnel could probably be used. In the case of the Langley tunnel, an alternate location just behind the first set of corner vanes downstream from the 7 ft × 10 ft test section was considered briefly as a possible test location (Fig. 4). Surveys of the velocity distribution at this location indicated that the flow was very distorted and unsteady due to flow separation from the tunnel walls upstream of this location. A very extensive screen installation would be needed to smooth out the flow but reports (such as Ref. 6) on screen installations indicate that a useful test facility could probably be achieved. Such a screen installation would absorb considerable power and would reduce the tunnel speed somewhat. In the case of the Langley 300 mph

7 ft × 10 ft tunnel, it was estimated that the top speed of the tunnel would be reduced by about 20%. Such a reduction in the top speed of most low-speed tunnels would not be considered serious, however, and would actually be considered a small penalty to pay as compared with building an entirely new tunnel for VTOL-STOL model testing.

5. CONCLUDING REMARKS

It has been shown that in wind-tunnel tests of VTOL and STOL configurations the tunnel wall can cause premature stall and loss of lift in addition to the usual wall effects. Several circumstances contribute to this premature stall. First, the propeller slipstream might strike the tunnel wall and be diverted by it, thereby altering the direction that the flow takes on leaving the trailing edge of the wing. This direction is usually such as to make it harder to maintain the Kutta condition and separation occurs. Secondly, the very large circulation lift generated with the aid of the jet flap or propeller slipstreams causes a much greater curvature of the streamlines than exists for power-off testing. The tunnel walls, however, establish the condition that the streamlines at the walls shall be straight. With the walls close to the model, this causes a considerable distortion of the streamlines in such a manner as to increase the adverse pressure gradient over the rear part of the wing which contributes to premature stall. Thirdly, with the jet-flap models and possibly with the propeller-driven models, lift losses may occur when a vortex type of flow develops under the wing.

Precise recommendations with regard to the ratio of model size to tunnel size cannot be given because of the scarcity of directly comparable data on this subject. However, recent experiences at the Langley Research Center suggest that for propeller-driven configurations the walls should be at least 4 or 5 propeller diameters from the model in order to avoid serious wall effects under static and very low-speed test conditions. Also, for tests at forward speeds with either propeller-driven or jet-flap models, the suggestion of Anscombe and Williams[3] that the model size be chosen so that the maximum expected increment of angle of attack due to induced upwash as calculated by conventional methods should not exceed about 2.0° appears to be reasonable.

REFERENCES

1. Kuhn, Richard E.
   Hayes, William C., Jr.
   Wind-Tunnel Investigation of Effect of Propeller Slipstreams on Aerodynamic Characteristics of a Wing Equipped With a 50-Percent-Chord Sliding Flap and a 30-Percent-Chord Slotted Flap. NACA TN 3918, 1957.

2. Kuhn, Richard E.
   Investigation of Effectiveness of a Wing Equipped With a 50-Percent-Chord Sliding Flap, a 30-Percent-Chord Slotted Flap, and a 30-Percent-Chord Slat in Deflecting Propeller Slipstreams Downward for Vertical Take-Off. NACA TN 3919, 1957.

3. Anscombe, A.
   Williams, J.
   Some Comments on High-Lift Testing in Wind Tunnels With Particular Reference to Jet-Blowing Models. Rep. 63, AGARD North Atlantic Treaty Organization (Brussels), Aug. 1956.

4. Lowry, John G.
   et alii
   The Jet-Augmented Flap. IAS Preprint No. 715 (presented at the 25th Annual Meeting of the Institute of the Aeronautical Sciences, Jan. 28-31, 1957).

5. Lockwood, Vernard E.
   et alii
   Wind-Tunnel Investigation of Jet-Augmented Flaps on a Rectangular Wing to High Momentum Coefficients. NACA TN 3865, 1956.

6. Schubauer, G.B.
   et alii
   Aerodynamic Characteristics of Damping Screens. NACA TN 2001, 1950.

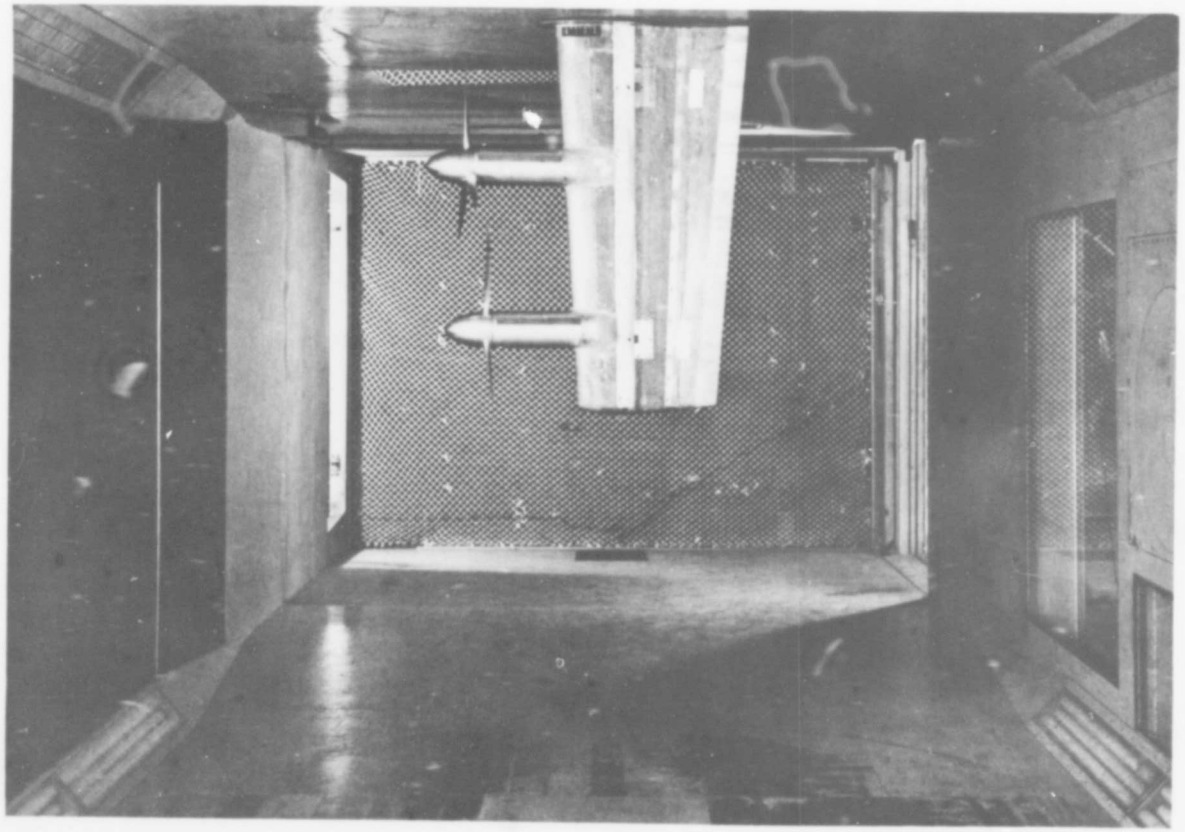

Fig.1 Deflected-slipstream model (flaps retracted) installed in NASA Langley 300 mph 7 ft x 10 ft tunnel

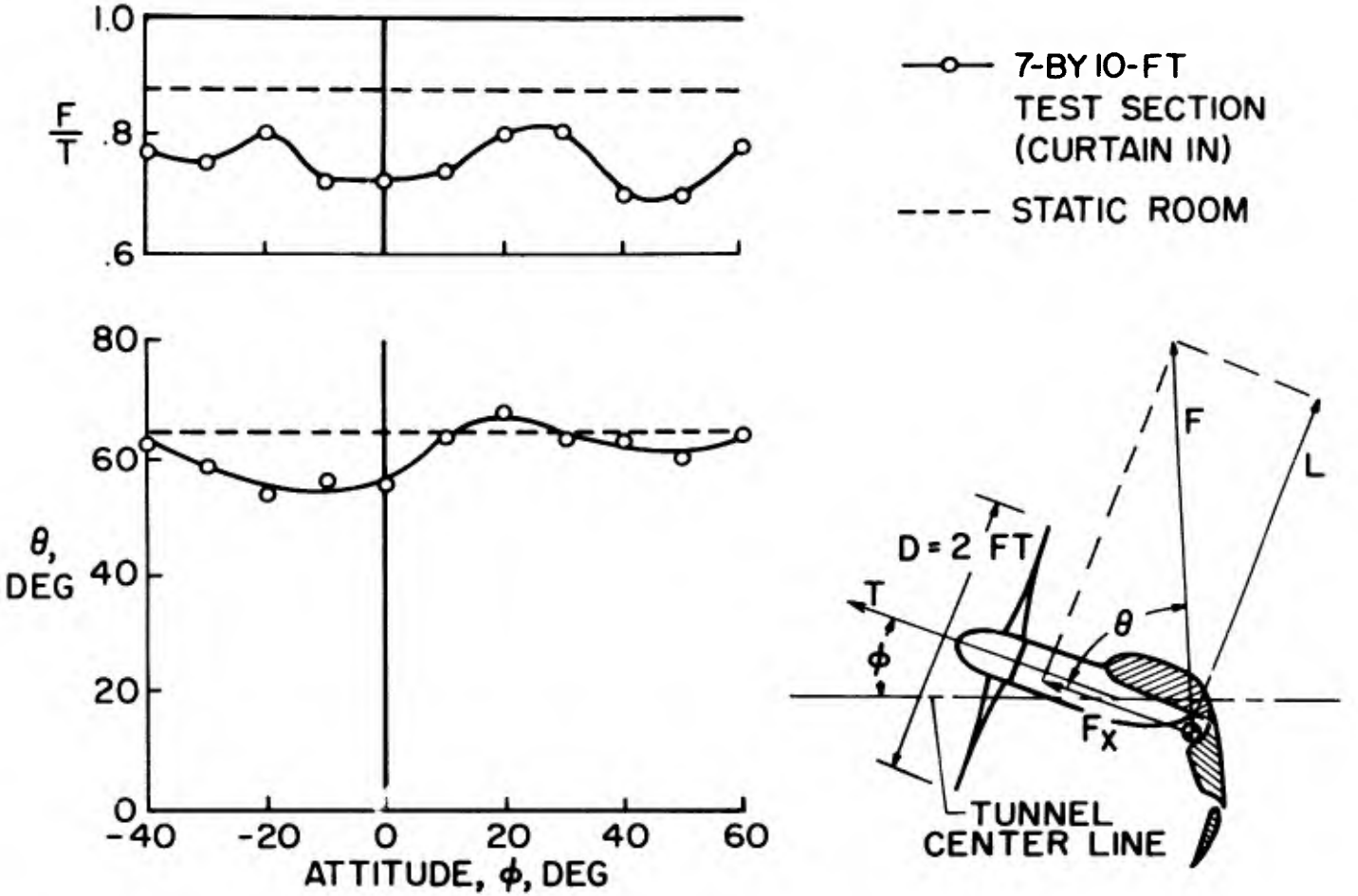

Fig.2 Slipstream deflection characteristics measured in the 7 ft x 10 ft test section

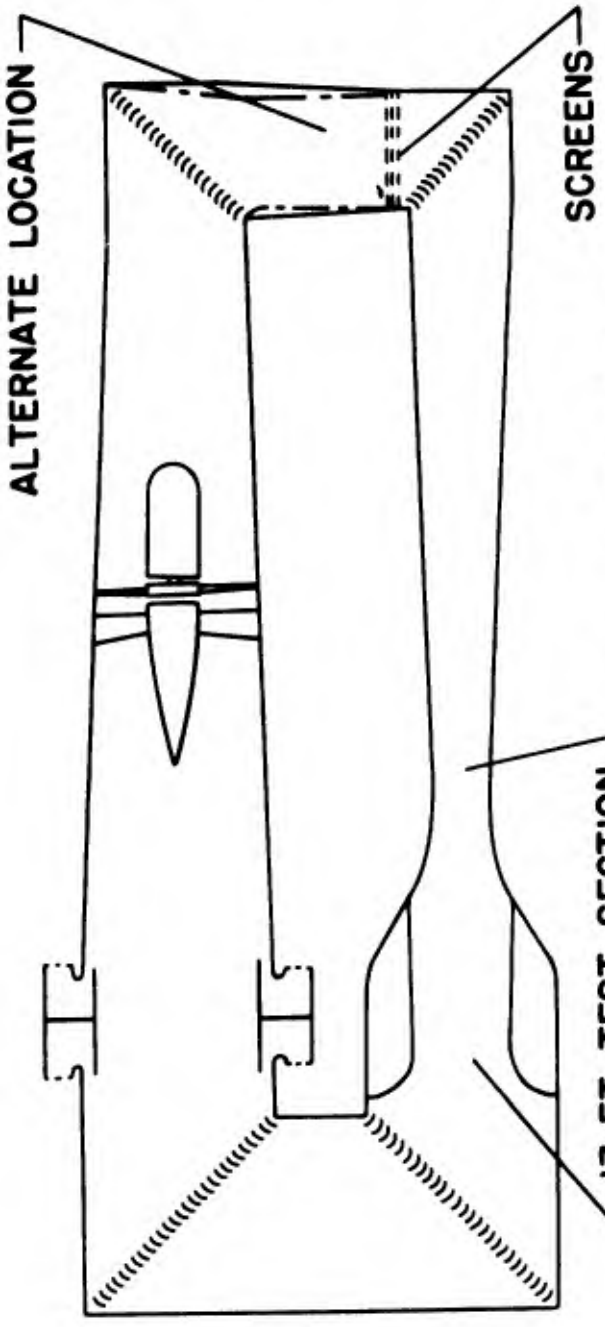

Fig.4 Installation of 17 ft test section in the NASA Langley 300 mph 7 ft x 10 ft tunnel

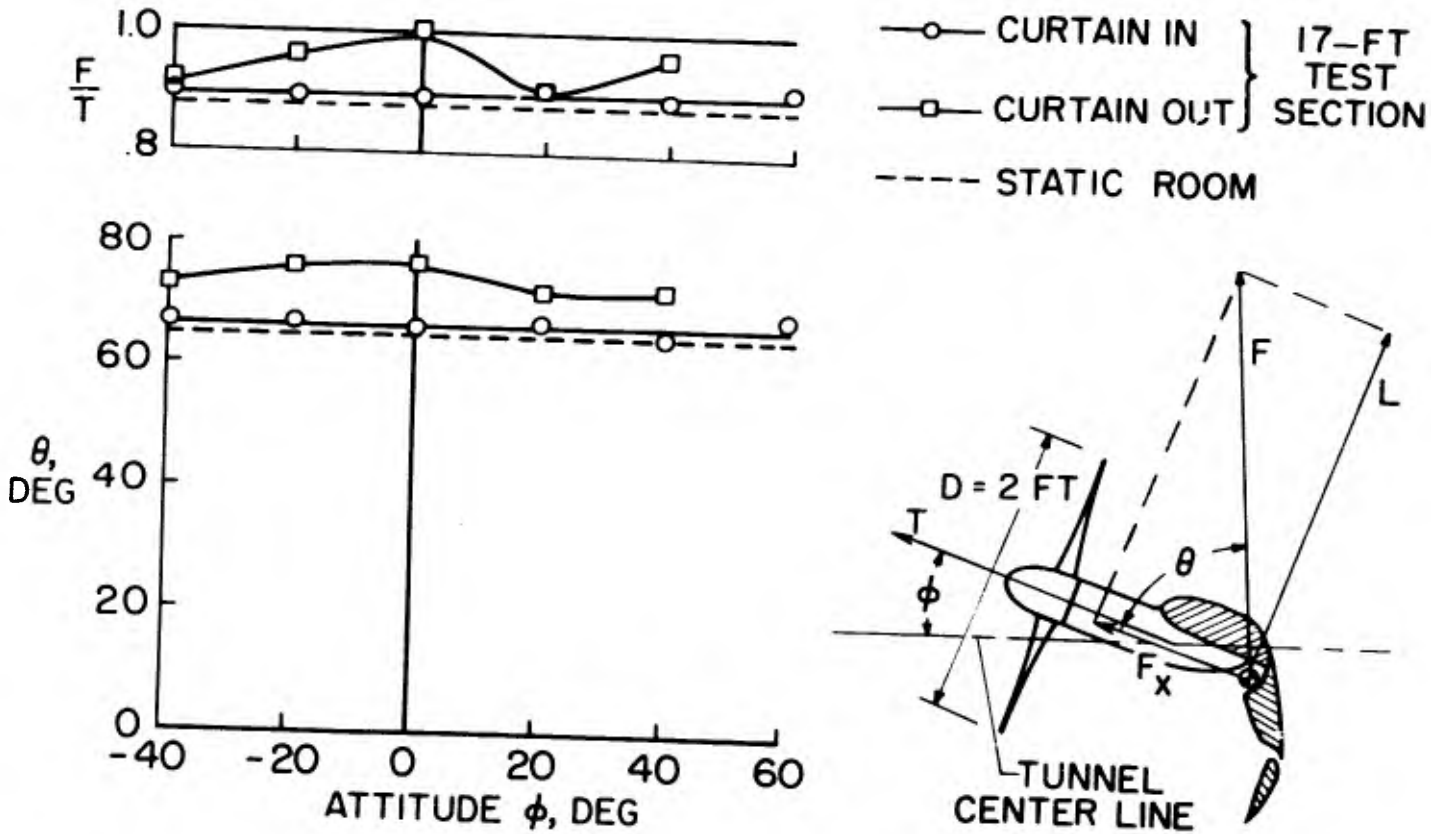

Fig.5 Slipstream deflection characteristics measured in the 17 ft test section

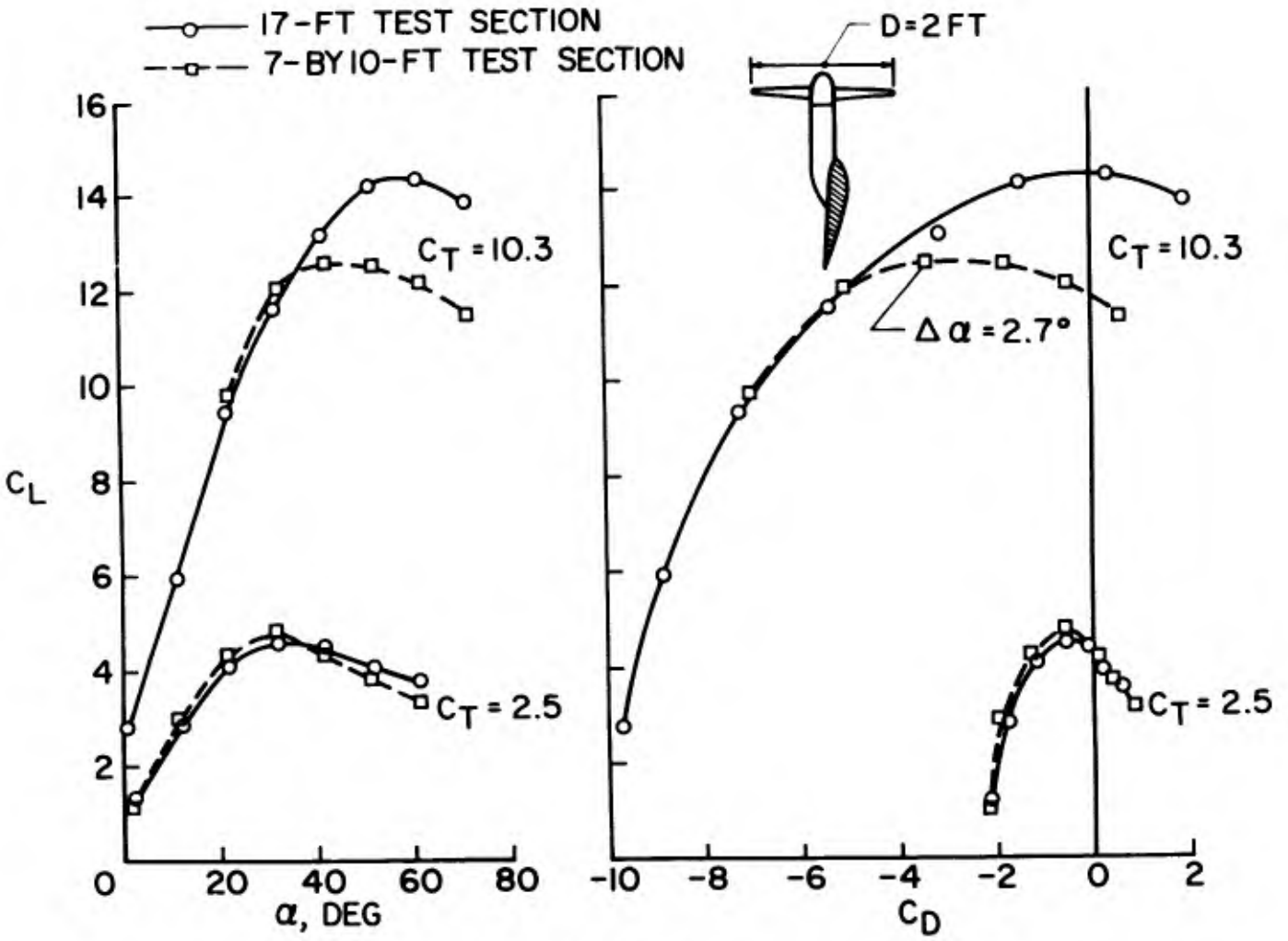

(a) Tilt-wing configuration

Fig.6 Effect of test section size on data obtained in transition speed range

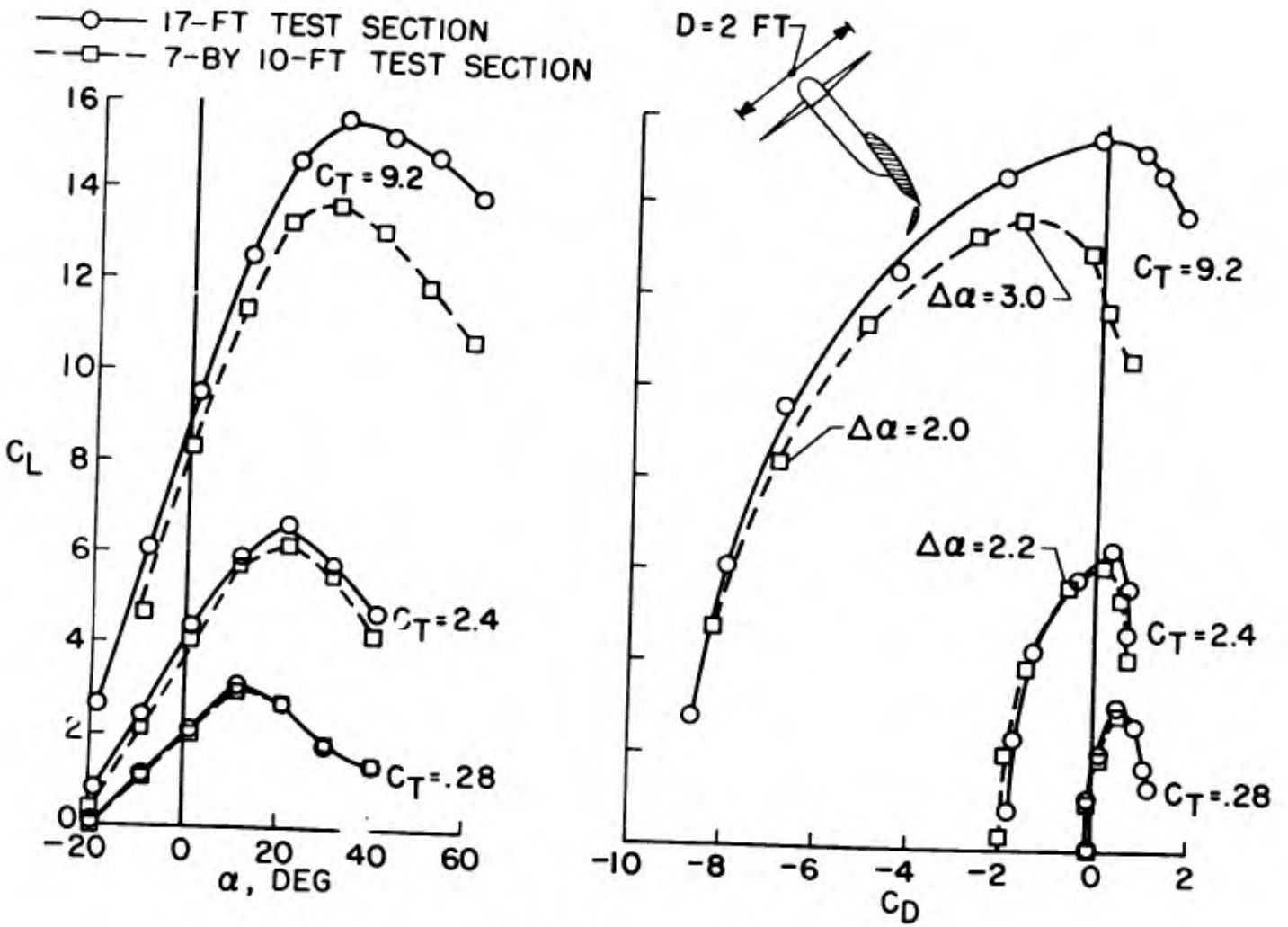

(b) Tilt-wing with flap

Fig.6 Effect of test section size on data obtained in transition speed range

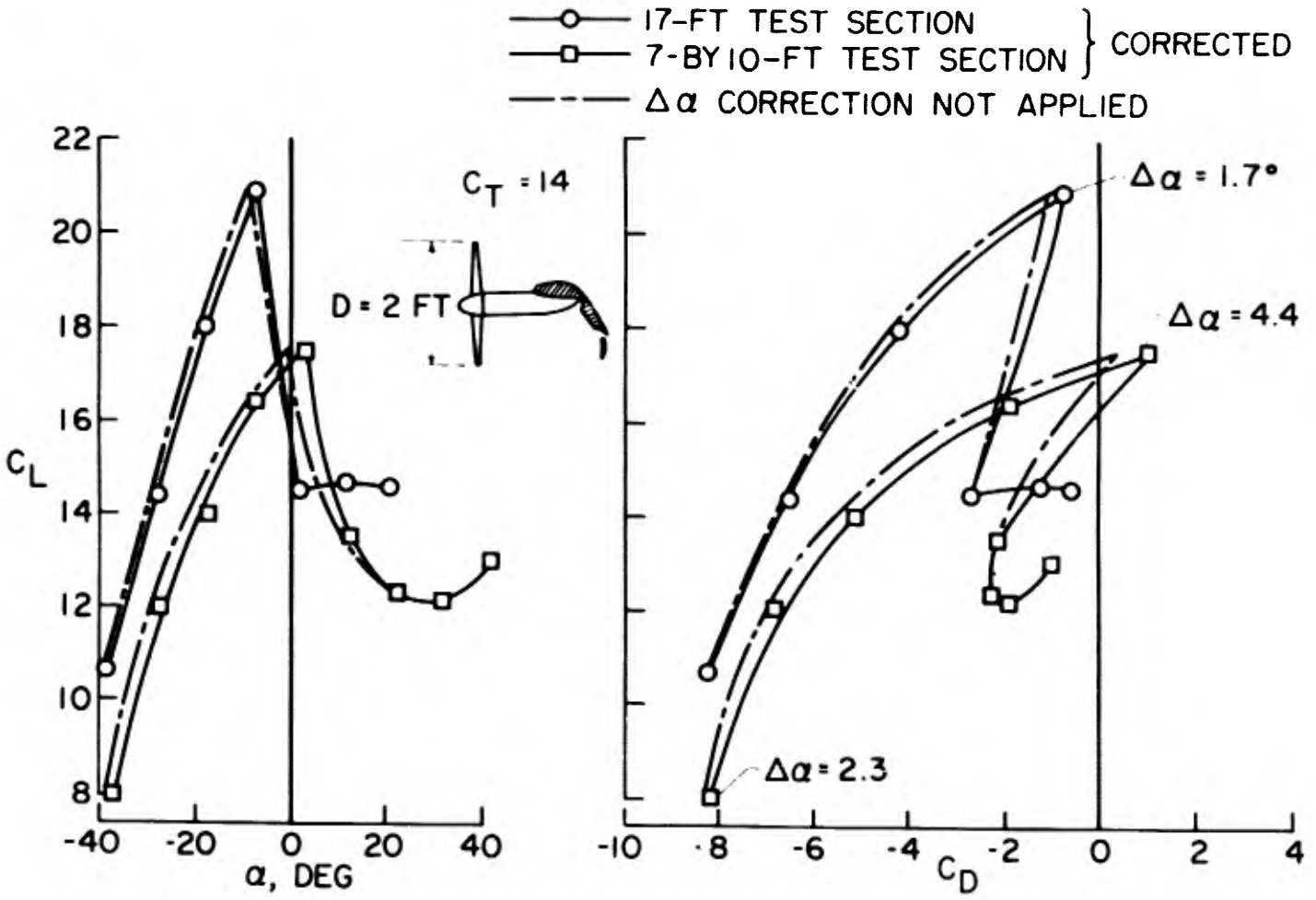

(c) Deflected-slipstream configuration

Fig.6 Effect of test section size on data obtained in transition speed range

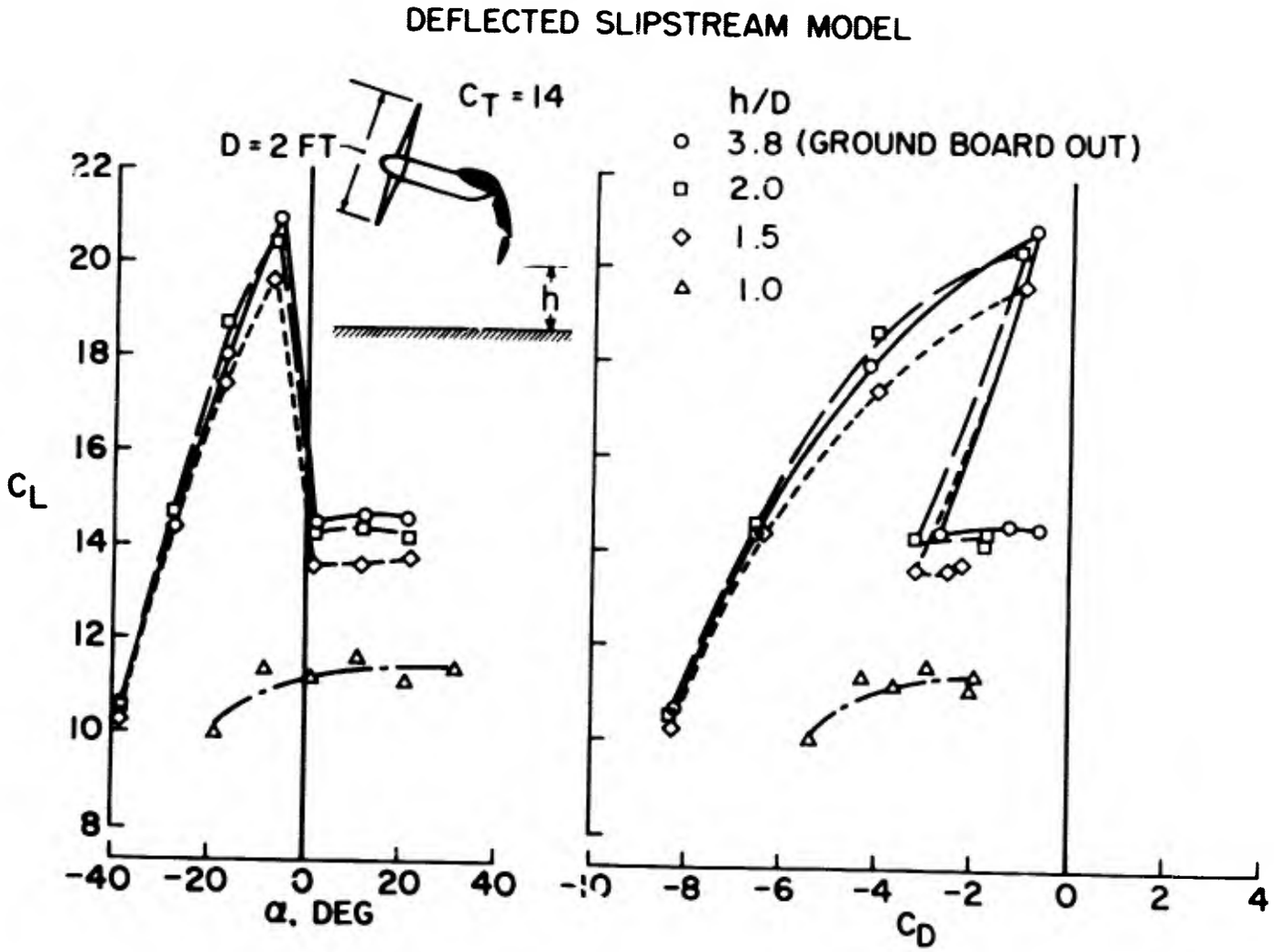

Fig.7 Effect of ground proximity

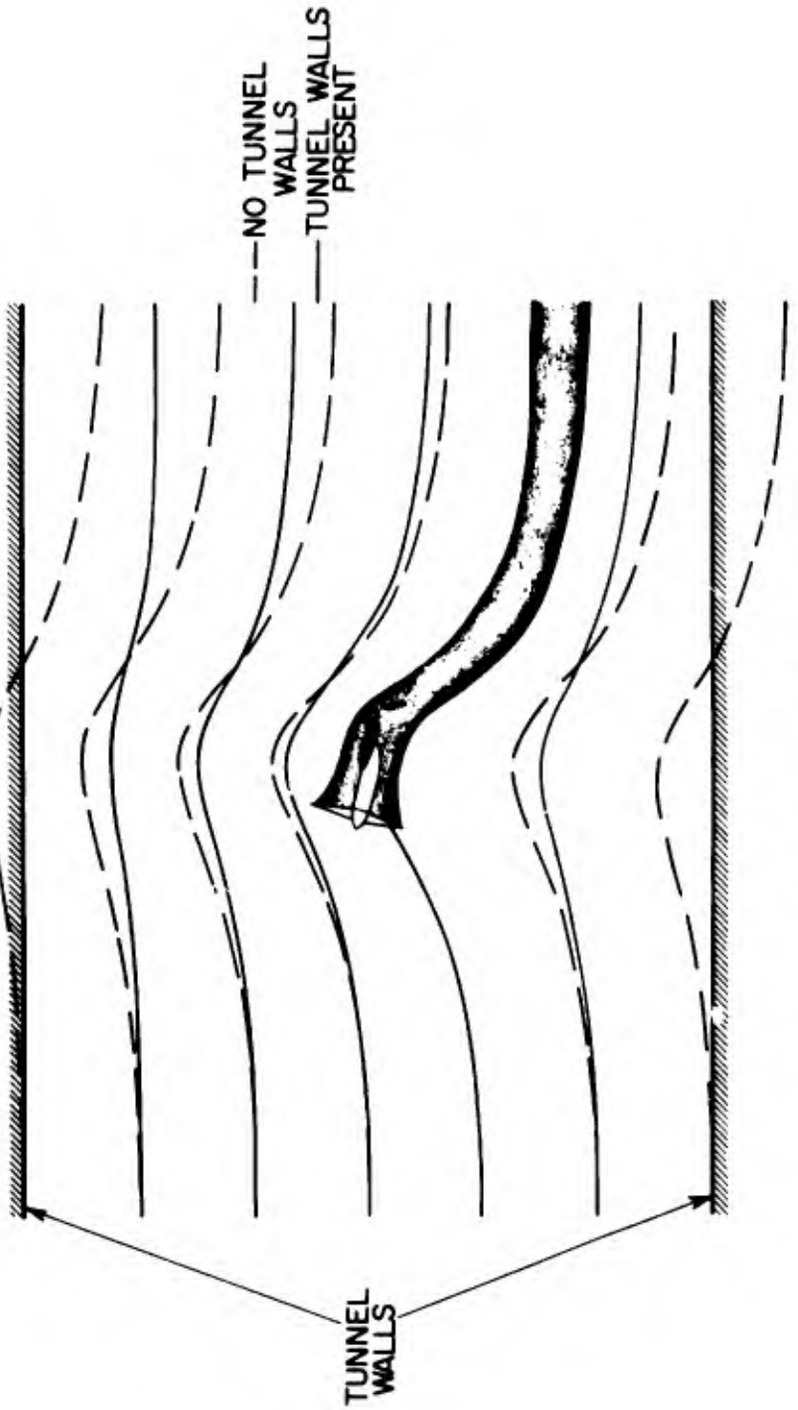

Fig.8 Effect of tunnel walls on flow about model

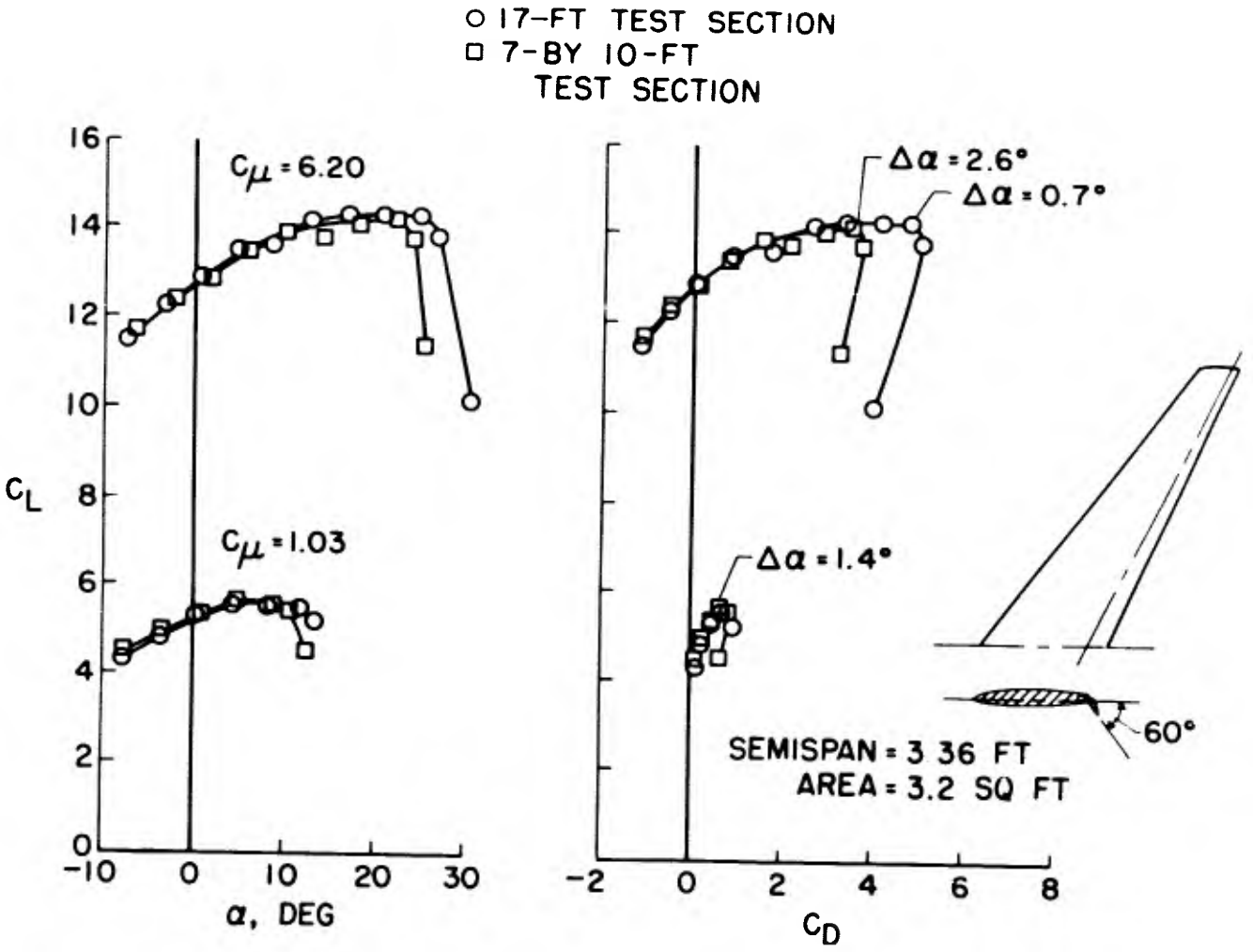

(a) Swept-wing model

Fig.9 Effect of test-section size, jet flap models

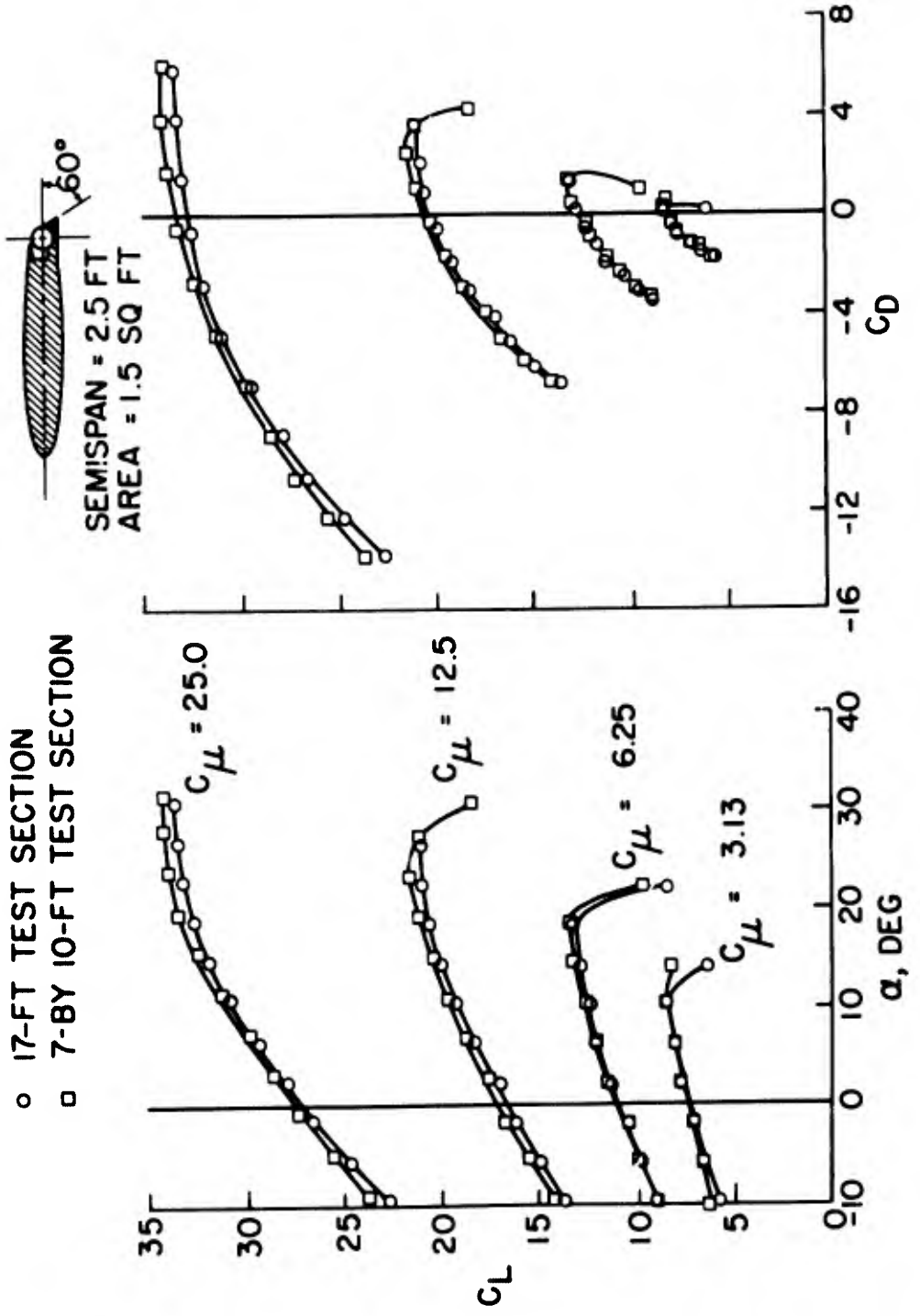

(b) Unswept-wing model

Fig.9 Effect of test-section size, jet flap models

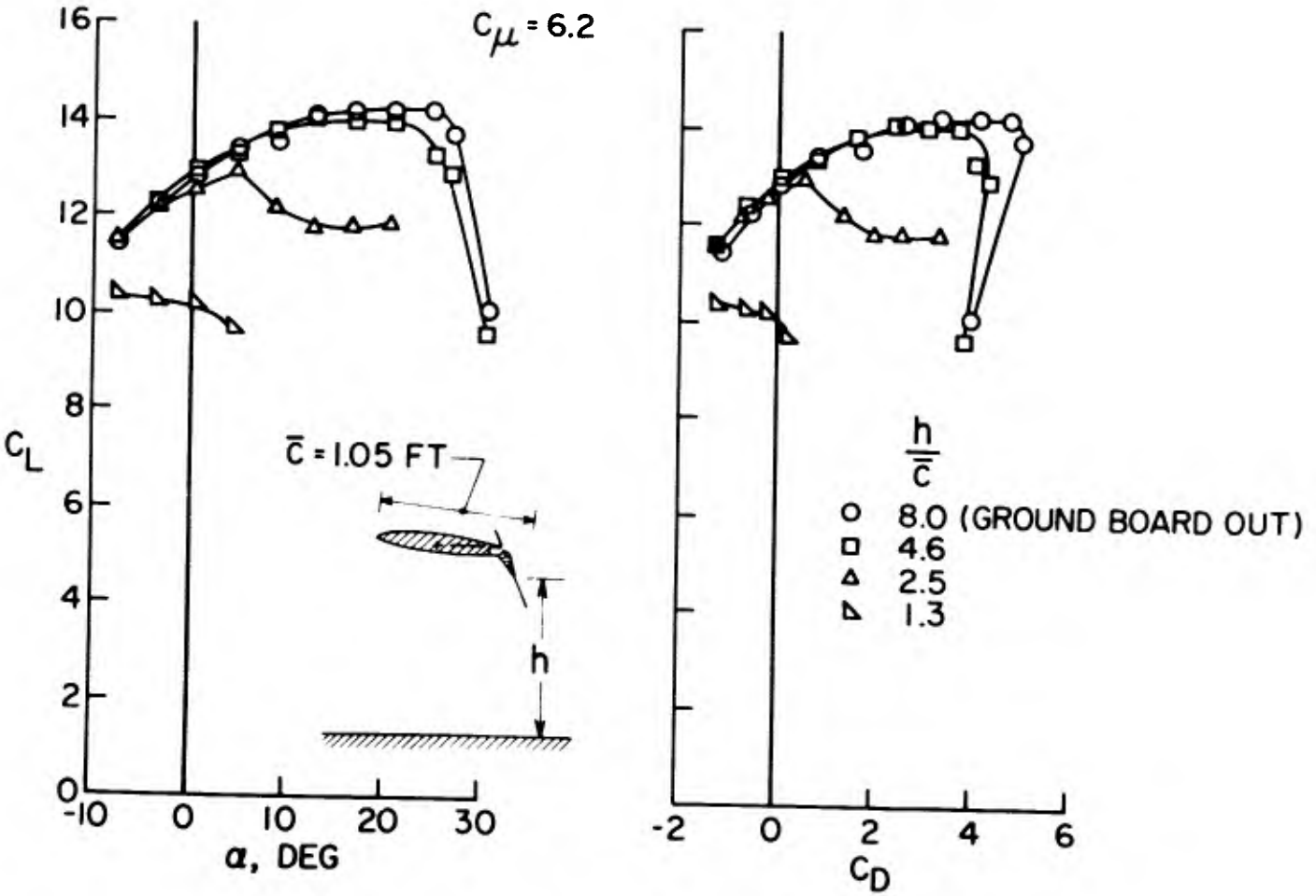

Fig. 10 Effect of ground proximity, swept-wing jet flap model

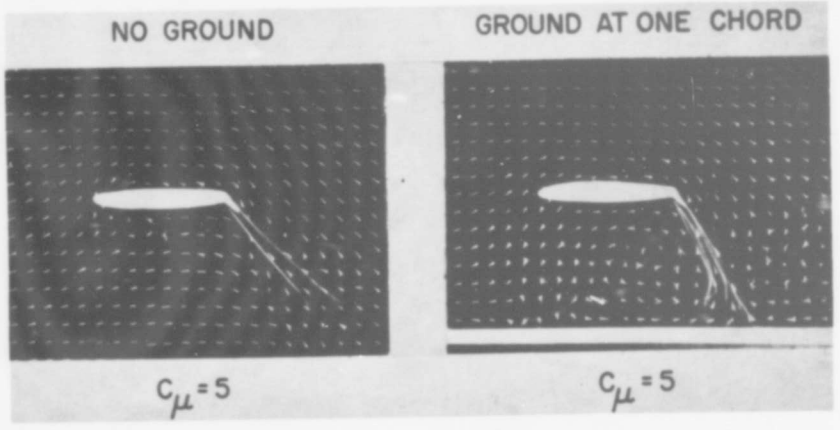

Fig.11 Effect of ground proximity on flow field about a wing with a jet flap

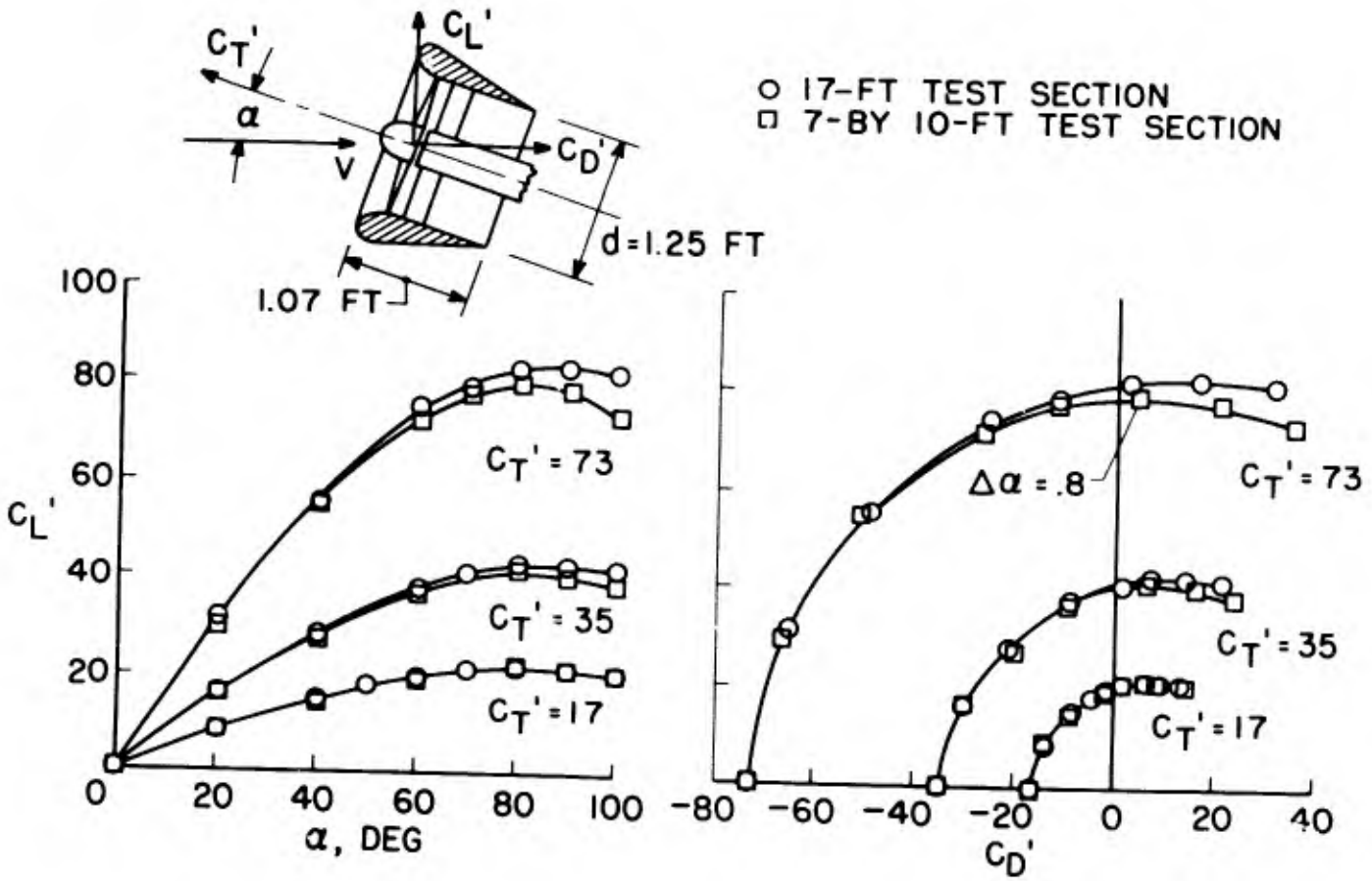

Fig.12 Comparison of data obtained on ducted fan in two test sections

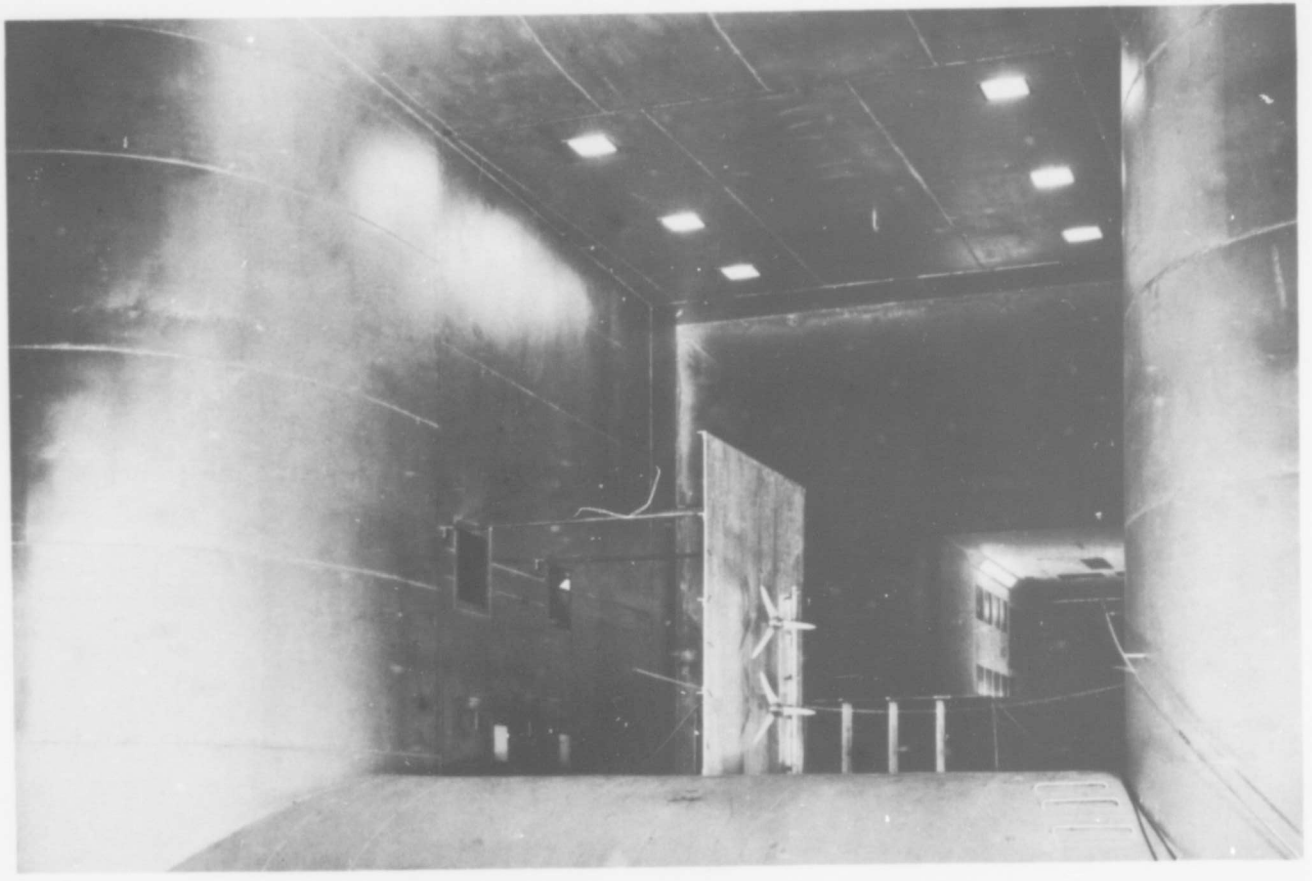

Fig.13 The 17 ft test section installed in NASA Langley 300 mph 7 ft x 10 ft tunnel

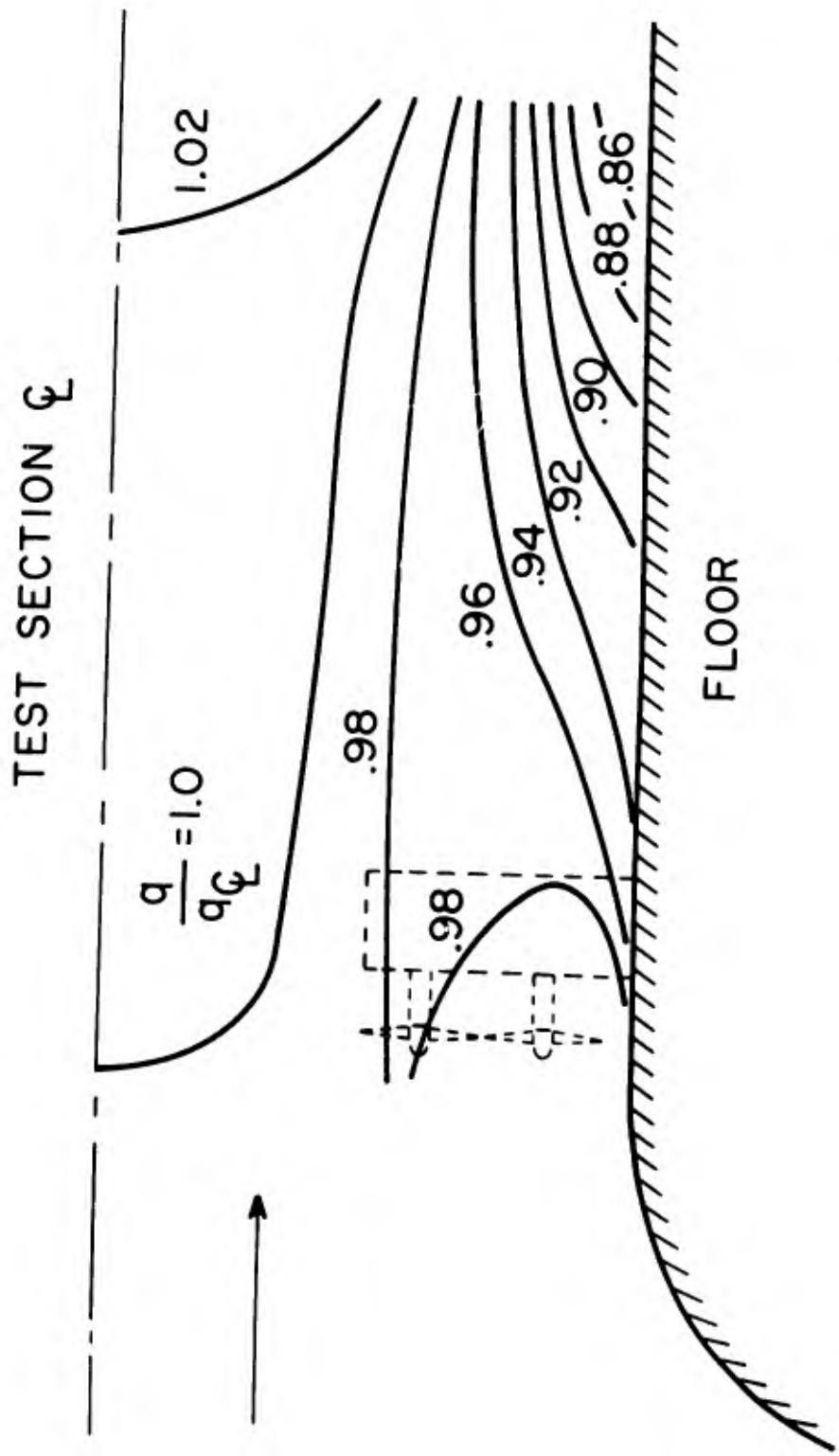

Fig.14 Contour lines of constant dynamic pressure in 17 ft test section